Supplemental Material: Separation scaling for viscous vortex reconnection

Jie Yao* and Fazle Hussain†
Department of Mechanical Engineering, Texas Tech University, Lubbock, TX 79409
(Dated: April 14, 2020)

SI.1: NUMERICAL METHODS

Direct numerical simulation is performed in the velocity-vorticity ($\mathbf{u}-\boldsymbol{\omega}$) form of the incompressible Navier-stokes equations

$$\nabla \cdot \mathbf{u} = 0, \tag{1}$$

$$\frac{\partial \boldsymbol{\omega}}{\partial t} + \mathbf{u} \cdot \nabla \boldsymbol{\omega} = \boldsymbol{\omega} \cdot \nabla \mathbf{u} + \nu \nabla^2 \boldsymbol{\omega} \tag{2}$$

where ν is the kinematic viscosity. DNS of these equations is carried out using a pseudospectral algorithm same as those in refs. [1, 2]. The domain decomposition and fast Fourier transform are performed using the open-source library "2DECOMP&FFT" [3], and 2/3 truncation rule is employed for dealiasing. Time integration is performed using the adaptive time-stepping with third-order low-storage Runge-Kutta scheme. In the current study, the vortices are assumed to have a Gaussian cross-section with vorticity distribution $\omega(r) = \Gamma/(4\pi r_0^2)\exp[-r^2/4r_0^2]$ with the circulation $\Gamma = 1$ and core scale $r_0 = 0.01$; and the Reynolds number Re_Γ is varied by changing the viscosity ν.

Colliding vortex rings

For this case, to suppress the symmetry-breaking (planar-jet) instability and reduce the computational cost, the symmetries of the initial condition are further employed – hence only a quarter of the domain ($L_x = 2L_y = 2L_z = 2\pi$) is simulated. The number of grid-points in the x, y and z directions are $N_x \times N_y \times N_z = 2048 \times 1025 \times 1025$ and $4096 \times 2049 \times 2049$ for $Re_\Gamma = 2000$ and 4000, respectively.

Orthogonal vortex tubes

Each of the vortex tubes is orientated in the x and y directions, respectively. The two vortices intersect the z-axis at $(0, 0, -\delta_0/2)$ and $(0, 0, +\delta_0/2)$. The initial separation is chosen the same as the colliding ring case, namely, $\delta_0 = 0.2$. The computational domain is is $\{[x_{\min} : x_{\max}] \times [y_{\min} : y_{\max}] \times [z_{\min} : z_{\max}]\} = \{[-\pi : \pi] \times [-\pi : \pi] \times [-\pi : \pi]\}$ with the grids points $N_x \times N_y \times N_z = 2048 \times 2048 \times 2048$ and $4096 \times 4096 \times 4096$ for $Re_\Gamma = 2000$ and 4000, respectively.

Vortex ring and tube interaction

The vortex ring is of radius $R = 1$ and centre at $(0, 0, -0.2)$ on a plane perpendicular to the z direction; the vortex tube is orientated in the x direction. The computational resolution is the same as the orthogonal vortex tubes simulations: the computational domain is is $\{[x_{\min} : x_{\max}] \times [y_{\min} : y_{\max}] \times [z_{\min} : z_{\max}]\} = \{[-\pi : \pi] \times [-\pi : \pi] \times [-\pi : \pi]\}$ with the grids points $N_x \times N_y \times N_z = 2048 \times 2048 \times 2048$ and $4096 \times 4096 \times 4096$ for $Re_\Gamma = 2000$ and 4000, respectively.

* jie.yao@ttu.edu
† fazle.hussain@ttu.edu

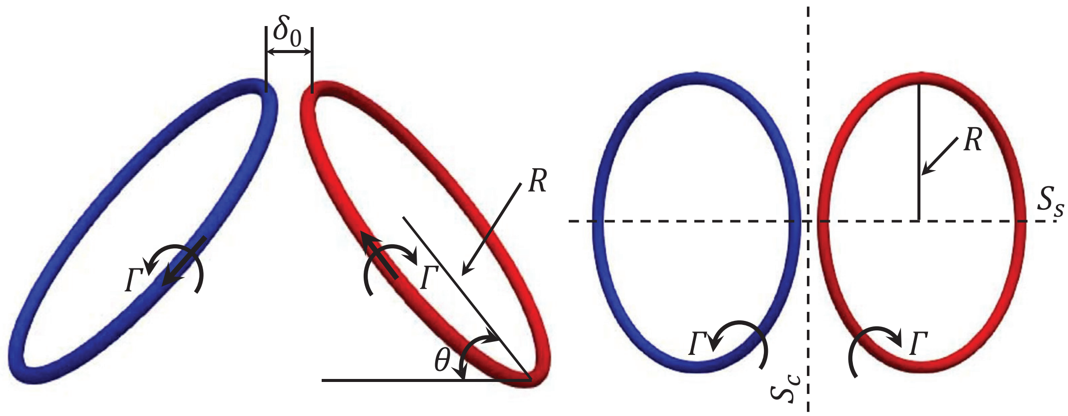

FIG. 1. The initial configuration of Reconnection for the colliding vortex rings. The vortex rings with circulation Γ and radius R are located on inclined plane with $\theta = \pi/4$ and initial minimum separation distance $\delta_0 = 0.2$; the right panel shows the corresponding top view with S_s and S_c denote the symmetry and collision planes respectively.

SI.2: VORTEX AXIS TRACKING

Colliding vortex rings

The initial configuration (Fig. 1) has two-fold symmetry regarding the symmetry S_s and collision S_c planes. Hence, the minimum distance δ between these two vortices occurs in the S_s and S_c planes for pre- and post-reconnection, respectively The vortices undergo significant core deformation into non-circular shapes when they approach (Fig. 2), and the reconnected vortex filaments take some time to collect together to form the bridge after reconnection (Fig. 3 –which makes the vortex center difficult to be determined. Following [2, 4], we take the vorticity centroid (computed as the centroid of ω_y which is above 75 % of its maximum) to be the vortex center. For example, for vortex in the symmetry ($y = 0$ plane, the center is defined as

$$\mathbf{x}_c = (x_c, 0, z_c) = \frac{\int_{x=-\pi}^{x=\pi} \int_{z=-\pi}^{z=0} \omega_y * \mathbf{x} dx dz}{\int_{x=-\pi}^{x=\pi} \int_{z=-\pi}^{z=0} \omega_y dx dz}. \tag{3}$$

The trajectories of the calculated vortex centers are represented as dashed lines in Figs. 2 and 3. Correspondingly, the minimum distance δ is the distance between the two vortex centers. In addition, the vortex lines that go through these centers can be considered as the vortex axis. Without loss of generality, and for sake of simplicity, we show in movie S2 the time evolution of the vortex axis (calculated using "stream3" function in Matlab) at $Re_\Gamma = 2000$; and the evolution at $Re_\Gamma = 4000$ are quantitatively the same.

Orthogonal vortex tubes

To determine the minimum distance between these two vortex tubes, the axis of the vortex tubes needs to be tracked. Here, we propose a vortex tracking method based on the vortex lines that go through the vortex center at the boundary. First, the centriod of the vortex tubes at the planes $x = -\pi$ and $y = -\pi$ is determined using same procedure discussed above (Eq. 3). Then, vortex lines that seeds from these two centers are integrated using the "stream3" function in Matlab. Fig. 4 (and Movie S4) shows the time evolution of the vortex axis for $Re_\Gamma = 2000$; and the evolution at $Re_\Gamma = 4000$ are quantitatively the same. Finally, the minimum separation distance δ is taken as the shortest distance between these two vortex lines. Note that the vortex axis and the corresponding δ depends on the choice of the seeds of the vortex lines. However, in the present work, we are mainly focused in the scaling of δ that is much large than the vortex core size; hence the variation of seeds points does not alter the scaling of δ in this regime.

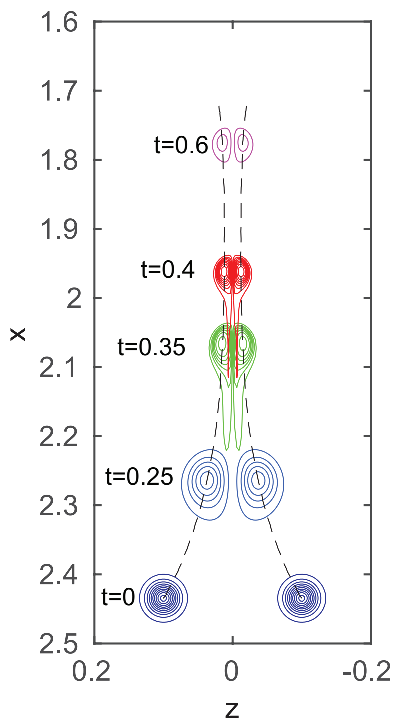

FIG. 2. Evolution of the vortex core shape (represented by the vorticity iso-contours $\omega_y = [0.05 : 0.1 : 2]\omega_0$) in the S_s plane for the colliding vortex rings at $Re_\Gamma = 2000$. The dash line denotes the vortex core trajectory.

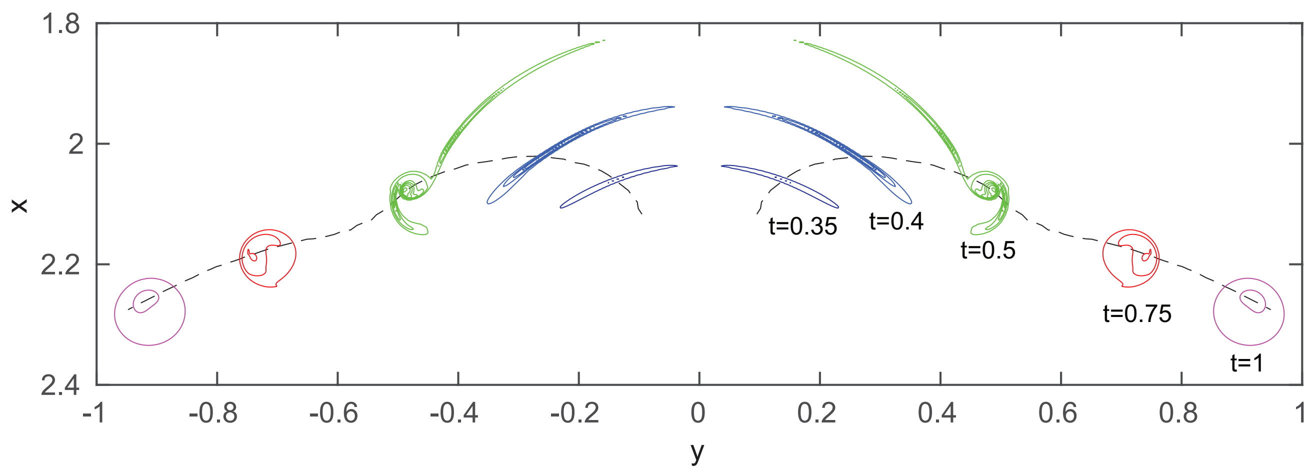

FIG. 3. Evolution of the vortex core (represented by the vorticity iso-contours $\omega_z = [0.05 : 0.1 : 2]\omega_0$) on the S_c plane for for the colliding vortex rings at $Re_\Gamma = 2000$. The dash line denotes the vortex core trajectory.

Vortex ring and tube interaction

Except for the choice of the seeds of the vortex lines, the vortex axis tracking algorithm for this configuration is the same as the case of the orthogonal vortex tubes. The geometry is symmetric with respect to $x = 0$ plane. Fig. 5 shows the vortex patches in the $x = 0$ plane. Three vortex patches exist in the $x = 0$ plane, with two of them are the same sign: one is from vortex ring and the other is from vortex tube. To unambiguously tracking the vortex ring and tube, the centroid of the two same-signed vortices in $x = 0$ plane are employed as the seeds of the vortex lines. The trajectory of these two same signed vortex patches are shown in Fig. 5, and they intersect with each other at $t = 1.1255$, after which parts of vortex ring and tube exchanges. Fig. 6 (and also Movie S6) shows the time evolution

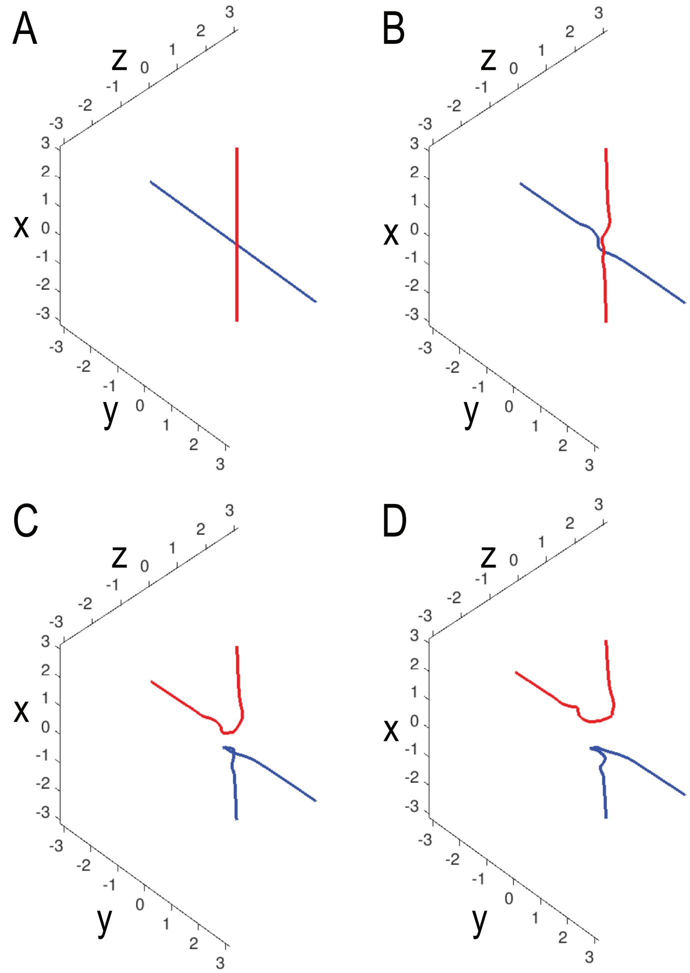

FIG. 4. Evolution of the vortex axis for the orthogonal vortex tubes case at $Re_\Gamma = 2000$.

of the vortex axis integrated from the vortex centroid in Fig. 5 for $Re_\Gamma = 2000$; and the evolution at $Re_\Gamma = 4000$ are quantitatively the same. It is clearly that the axis of vortex rings and tube can be unambiguously identified.

MOVIES

Movie S1: Evolution of flow structures for reconnection of colliding vortex rings at $Re_\Gamma = 2000$ using direct numerical simulation of Naiver-Stokes equation. The radius of the vortex ring is $R = 1$ and the initial minimum distance between two rings is $\delta_0 = 0.2$. The flow structures are represented by vorticity isosurface at 5% of maximum initial vorticity $|\boldsymbol{\omega}| = 0.05\omega_0$.

Movie S2: Evolution of vortex axis for reconnection of colliding vortex rings at $Re_\Gamma = 2000$ using vortex axis tracking algorithm developed in SI.2.

Movie S3: Evolution of flow structures for reconnection of orthogonal straight vortex tubes at $Re_\Gamma = 2000$ using direct numerical simulation of Naiver-Stokes equation. The initial separation between these two tubes is $\delta_0 = 0.2$. The flow structures are represented by vorticity isosurface at 5% of maximum initial vorticity $|\boldsymbol{\omega}| = 0.05\omega_0$.

Movie S4: Evolution of vortex axis for reconnection of orthogonal straight vortex tubes at $Re_\Gamma = 2000$ using vortex axis tracking algorithm developed in SI.2.

Movie S5: Evolution of flow structures for reconnection of vortex ring with a straight tube at $Re_\Gamma = 2000$ using direct numerical simulation of Naiver-Stokes equation. The radius of the vortex ring is $R = 1$ and the initial minimum distance is $\delta_0 = 0.4$. The flow structures are represented by vorticity isosurface at 5% of maximum initial vorticity $|\boldsymbol{\omega}| = 0.05\omega_0$.

Movie S6: Evolution of vortex axis for reconnection of vortex ring with a straight tube at $Re_\Gamma = 2000$ using vortex

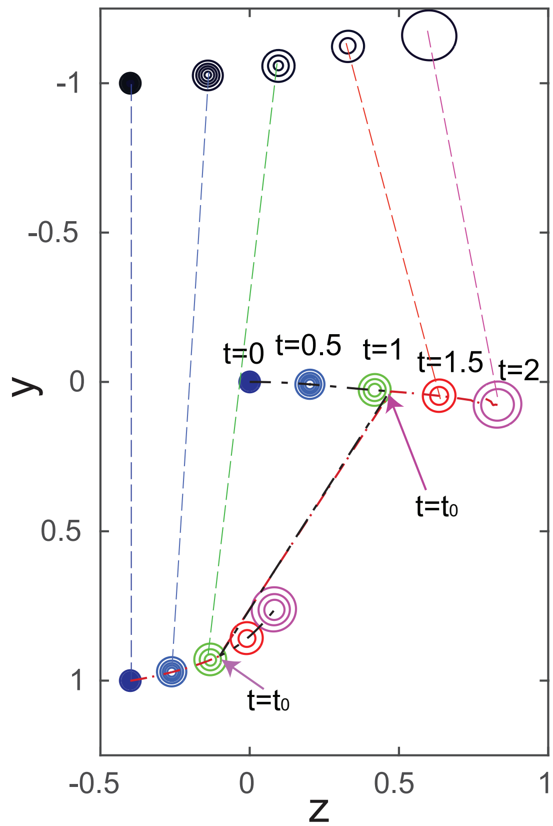

FIG. 5. Evolution of the vortex patches (represented by vorticity iso-contours $|\omega_x| = [0.05 : 0.05 : 2]\omega_0$ in $x = 0$ plane for the interaction of vortex ring and tube at $Re_\Gamma = 2000$. The two vortex patches that are connected by dashed lines denotes the the vortex dipole of the ring; and red and black dotted dash lines represents the trajectories of the negative ω_x patches of the vortex rings and tube, respectively. Note that the trajectories intersect at $t = 1.1255$.

axis tracking algorithm developed in SI.2.

[1] J. Yao and F. Hussain, A physical model of turbulence cascade via vortex reconnection sequence and avalanche, Journal of Fluid Mechanics **883** (2020).

[2] J. Yao and F. Hussain, On singularity formation via viscous vortex reconnection, Journal of Fluid Mechanics **888** (2020).

[3] N. Li and S. Laizet, 2decomp & fft-a highly scalable 2d decomposition library and fft interface, in *Cray User Group 2010 conference* (2010).

[4] F. Hussain and K. Duraisamy, Mechanics of viscous vortex reconnection, Physics of Fluids **23**, 021701 (2011).

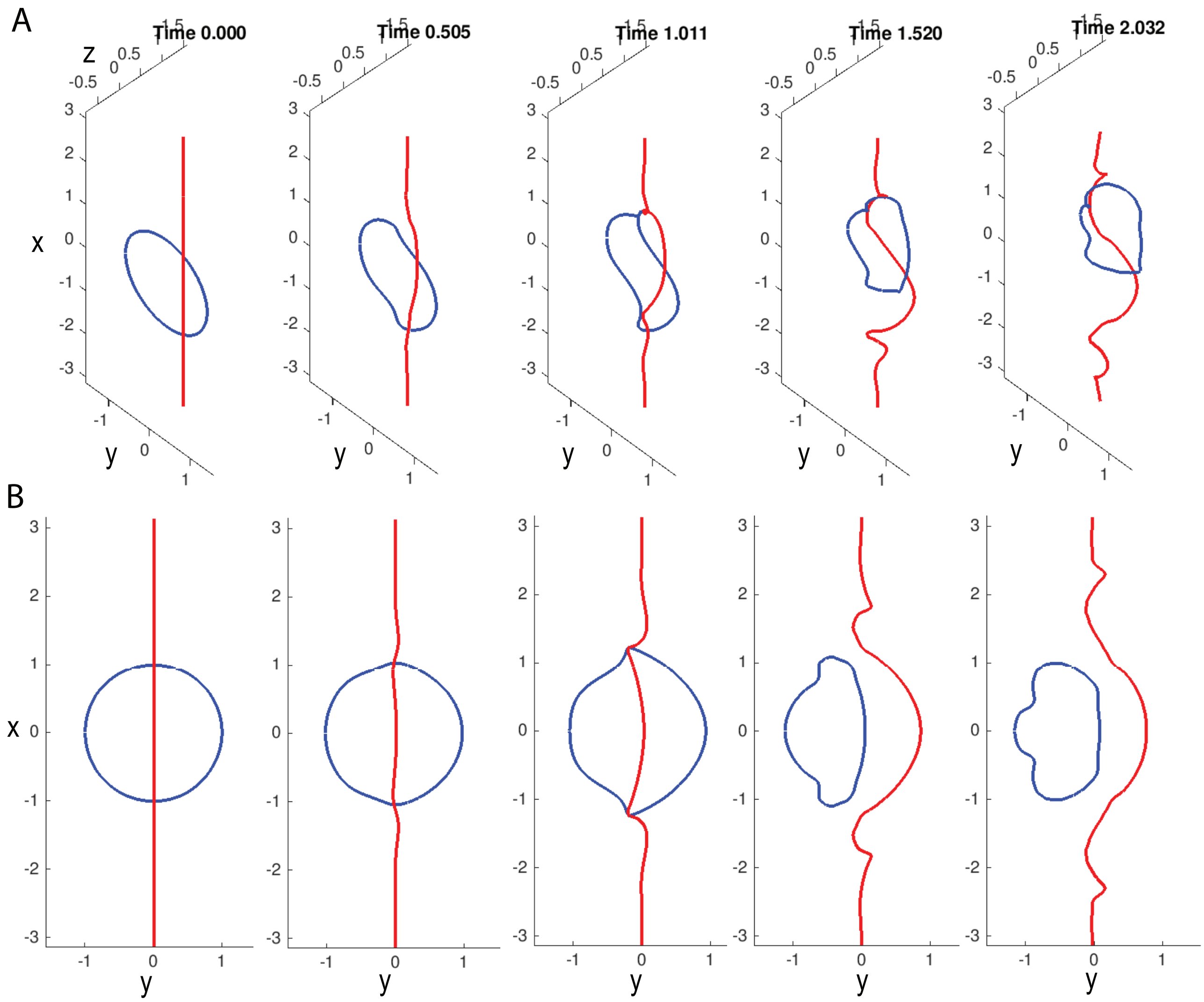

FIG. 6. Evolution of the vortex axis for reconnection of the vortex ring (blue) and tube (red) at $Re_\Gamma = 2000$: (A) 3D and (B) side view.